AMERICAN SOCIETY FOR MICROBIOLOGY | Infection and Immunity®

HOST-ASSOCIATED MICROBIAL COMMUNITIES

# Dysbiosis of Inferior Turbinate Microbiota Is Associated with High Total IgE Levels in Patients with Allergic Rhinitis

**Dong-Wook Hyun,[a,b] Hyun Jin Min,[c] Min-Soo Kim,[a,b] Tae Woong Whon,[a,b] Na-Ri Shin,[a,b] Pil Soo Kim,[a,b] Hyun Sik Kim,[a,b] June Young Lee,[a,b] Woorim Kang,[a,b] Augustine M. K. Choi,[d] Joo-Heon Yoon,[e] Jin-Woo Bae[a,b]**

[a]Department of Life and Nanopharmaceutical Science, Kyung Hee University, Seoul, Republic of Korea

[b]Department of Biology, Kyung Hee University, Seoul, Republic of Korea

[c]Department of Otorhinolaryngology-Head and Neck Surgery, Chung-Ang University College of Medicine, Seoul, Republic of Korea

[d]Division of Pulmonary and Critical Care Medicine, Joan and Sanford I. Weill Department of Medicine, Weill Cornell Medicine, New York, New York, USA

[e]Department of Otorhinolaryngology, Yonsei University College of Medicine, Seoul, Republic of Korea

**ABSTRACT** Abnormalities in the human microbiota are associated with the etiology of allergic diseases. Although disease site-specific microbiota may be associated with disease pathophysiology, the role of the nasal microbiota is unclear. We sought to characterize the microbiota of the site of allergic rhinitis, the inferior turbinate, in subjects with allergic rhinitis ($n = 20$) and healthy controls ($n = 12$) and to examine the relationship of mucosal microbiota with disease occurrence, sensitized allergen number, and allergen-specific and total IgE levels. Microbial dysbiosis correlated significantly with total IgE levels representing combined allergic responses but not with disease occurrence, the number of sensitized allergens, or house dust mite allergen-specific IgE levels. Compared to the populations in individuals with low total IgE levels (group $IgE^{low}$), low microbial biodiversity with a high relative abundance of *Firmicutes* phylum (*Staphylococcus aureus*) and a low relative abundance of *Actinobacteria* phylum (*Propionibacterium acnes*) was observed in individuals with high total serum IgE levels (group $IgE^{high}$). Phylogeny-based microbial functional potential predicted by the 16S rRNA gene indicated an increase in signal transduction-related genes and a decrease in energy metabolism-related genes in group $IgE^{high}$ as shown in the microbial features with atopic and/or inflammatory diseases. Thus, dysbiosis of the inferior turbinate mucosa microbiota, particularly an increase in *S. aureus* and a decrease in *P. acnes*, is linked to high total IgE levels in allergic rhinitis, suggesting that inferior turbinate microbiota may be affected by accumulated allergic responses against sensitized allergens and that site-specific microbial alterations play a potential role in disease pathophysiology.

**KEYWORDS** inferior turbinate, nasal mucosa, commensal microbiota, immunoglobulin E, multiple-allergen simultaneous test, skin prick test, allergic rhinitis, *Staphylococcus aureus*, *Propionibacterium acnes*

Allergic rhinitis (AR) is a nasal allergic disease characterized by nasal hyperresponsiveness, immunoglobulin E (IgE) production, skewing of mucosal immune homeostasis toward a $T_H2$-type response, and accumulation of eosinophils and mast cells (1, 2). AR is a global health problem affecting 25% of the general population, and its worldwide prevalence has steadily increased over recent decades (3). Intriguingly, the epidemic is related to increased urbanization, a westernized diet, and overuse of antibiotics (4). The modern lifestyle reduces exposure to microbes and foreign antigens, which subsequently increases susceptibility to allergic diseases (5). This high incidence of allergic diseases is attributed to immature development of, and/or an imbalanced

**Received** 19 December 2017 **Returned for modification** 18 January 2018 **Accepted** 30 January 2018

**Accepted manuscript posted online** 5 February 2018

**Citation** Hyun D-W, Min HJ, Kim M-S, Whon TW, Shin N-R, Kim PS, Kim HS, Lee JY, Kang W, Choi AMK, Yoon J-H, Bae J-W. 2018. Dysbiosis of inferior turbinate microbiota is associated with high total IgE levels in patients with allergic rhinitis. Infect Immun 86:e00934-17. https://doi.org/10.1128/IAI.00934-17.

**Editor** Manuela Raffatellu, University of California San Diego School of Medicine



Address correspondence to Joo-Heon Yoon, jhyoon@yuhs.ac, or Jin-Woo Bae, baejw@khu.ac.kr.

D.-W.H., H.J.M., and M.-S.K. contributed equally to this article.

antigen response by, the host immune system, a process that relies on cross talk between host systems and the resident microbiota (6, 7).

The human body is densely populated by complex microbial communities, referred to as the microbiota. Genetic and environmental factors shape distinct communities of microbes at different body sites (8, 9). The microbiota plays a crucial role in host immunity (10). Disturbance or loss of the microbiota, termed dysbiosis, correlates with asthma and atopic dermatitis (11, 12). Accordingly, abnormalities in the microbiota and their subsequent effects on the immune system have attracted much attention. Several studies demonstrate that the commensal microbiota regulates susceptibility to allergic diseases. The absence of commensal bacteria augments basophil proliferation, increases the total number of infiltrating lymphocytes and eosinophils, exacerbates $T_H2$ cell responses and allergic inflammation, and reduces the number of ROR$\gamma t^+$ regulatory T cells (Tregs) and $T_H17$ cells (6, 13). Conversely, administration of *Lactobacillus* strains to germfree mice induces a $T_H1$-mediated immune response and ameliorates $T_H2$-related cytokine production and allergic sensitization (14). Furthermore, dysbiosis of the microbiota increases susceptibility to allergic diseases. Antibiotic-induced dysbiosis of the gut microbiota promotes food allergies and allergic airway inflammation in peanut allergen- and papain-induced allergy models, respectively (15, 16). Therefore, disruption of the microbe-host immune system interactions might be a primary cause of allergic disease. However, the role of alterations in the microbiota in allergic diseases has been highlighted only for the gut; the role played by the commensal microbiota in the nasal cavity in the development of AR has not been determined.

The inferior turbinates are the first line of immunological defense against external environmental irritants (17). The inferior turbinates become persistently enlarged in chronic AR patients, whereas they return to their normal size in healthy individuals. This mucosal enlargement increases epithelial permeability by stretching intercellular tight junctions (18) and induces cytokine secretion from ciliated cells or goblet cells, which eventually alters airway epithelial phenotypes (19). These epithelial phenotypes result in abnormal liquid accumulation at the airway surface, which, in turn, may affect the commensal microbiota in the nasal mucosa. In this regard, the local microbiota interacts closely with the local immune system and may have a direct effect on pathophysiology at the disease site; however, the association between the commensal microbiota at the disease site and AR pathogenesis is unknown.

This study aimed to identify the community structure, composition, and functional potential of the commensal microbiota in the inferior turbinate mucosae of AR patients and healthy subjects using 16S rRNA gene-based 454 pyrosequencing. The results suggest that total IgE levels representing combined allergic responses against all sensitized allergens, rather than AR occurrence or individual allergen-specific IgE levels, affect the composition and functional potential of the inferior turbinate mucosa microbiota.

## RESULTS

**Comparison of the inferior turbinate mucosa microbiota between AR and healthy subjects.** In this study, inferior turbinate mucosa samples (depicted in Fig. 1A) and clinical data from a total 32 participants were used. Criteria for participant enrollment and AR diagnosis and group categorizations for each comparison are shown in Fig. S1. 16S rRNA gene sequencing of inferior turbinate mucosa samples yielded 100,943 high-quality reads (3,145 $\pm$ 57 reads per sample). To investigate the effect of AR on the inferior turbinate microbiota, participants were first divided into two groups according to AR occurrence: one group was diagnosed with AR ($n = 20$; skin prick test [SPT] positive and multiple-allergen simultaneous test [MAST] positive; group AR+), whereas the other comprised healthy subjects with no AR ($n = 12$; SPT negative and MAST negative; group AR−) (Table 1; see also Table S1 in the supplemental material). We found no significant differences in inferior turbinate microbial community (Fig. S2A and B), diversity (Fig. S2C), or functional potential (Fig. S2F and G) between the AR+ and AR− groups, although we did find differences in the relative abundances of several

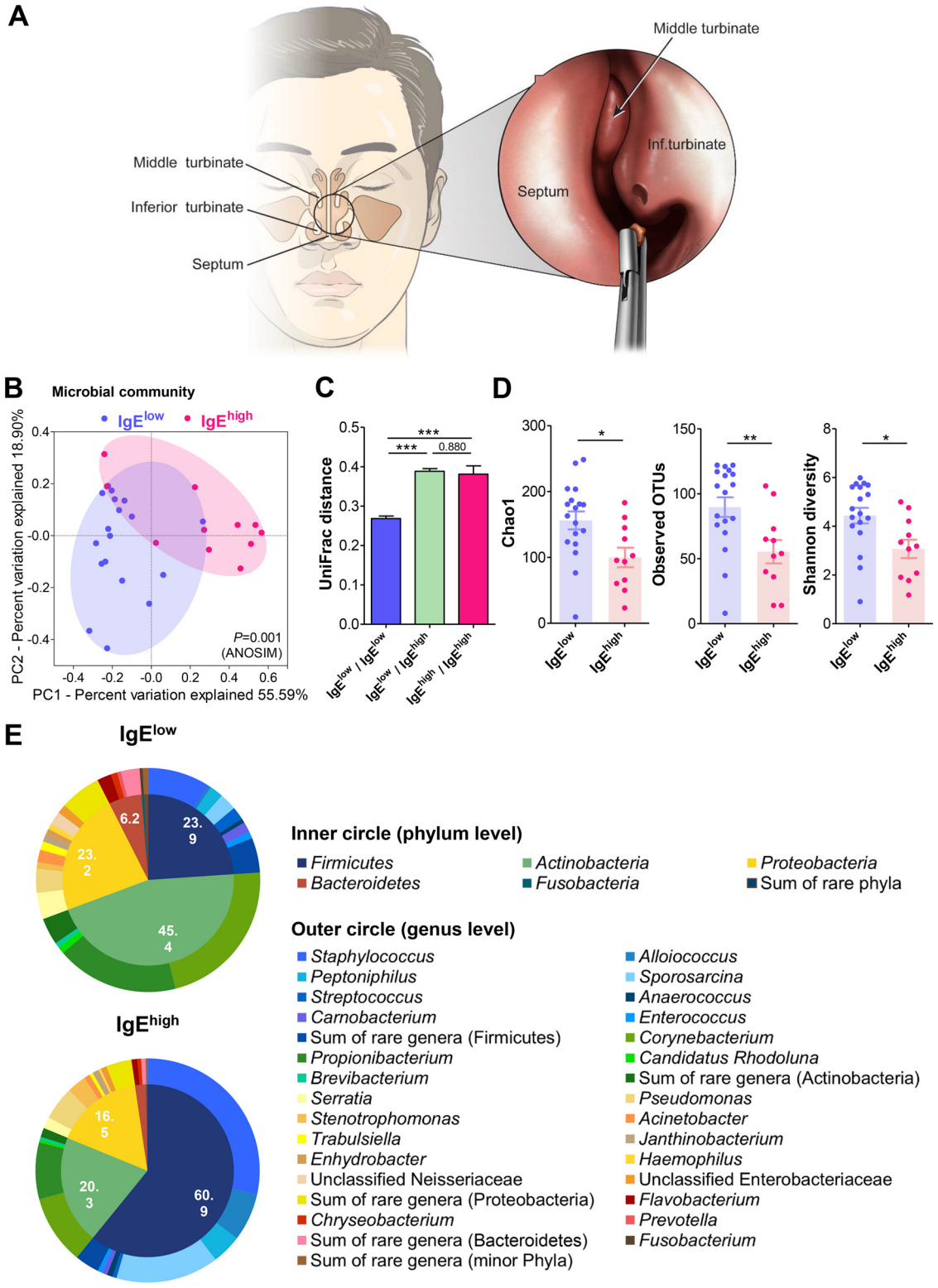


**FIG 1** Effect of immunoglobulin E (IgE) levels on the inferior turbinate mucosa microbiota and microbial diversity and community composition. (A) Schematic drawing showing harvesting of nasal mucosa from the inferior nasal turbinate. (B) Principal-coordinate analysis of weighted UniFrac distances of the inferior turbinate mucosa microbiota. Each point represents an individual microbiota. (C) Average weighted UniFrac distances representing intragroup and intergroup variability within the microbiota. (D) Comparison of alpha-diversity indices between IgE levels. Bars and dots represent the average diversity index score and diversity index score, respectively, for each sample. (E) Mean relative abundances of bacterial phyla (inner circles) and genera (outer circles) in groups $IgE^{low}$ and $IgE^{high}$. Only taxonomic groups at >0.5% of the total microbiota are shown. For panels C and D, *P* values were calculated by two-tailed Mann-Whitney *U* test. *, $P < 0.05$; **, $P < 0.01$; ***, $P < 0.001$.

**TABLE 1** Subject characteristics

| Parameter | Value for subject group[c] | | | |
|---|---|---|---|---|
| | Allergic rhinitis ($AR^+$) | Healthy ($AR^-$) | IgE level 3 ($IgE^{high}$) | IgE level 1 ($IgE^{low}$) |
| No. of subjects[a] | 20 | 12 | 11 | 18 |
| Male (%) | 16 (80.0) | 8 (66.7) | 10 (90.9) | 11 (61.1) |
| Female (%) | 4 (20.0) | 4 (33.3) | 1 (9.1) | 7 (38.8) |
| $SPT^+$ and $MAST^+$ (%) | 20 (100) | | 10 (90.9) | 8 (44.4) |
| $SPT^-$ and $MAST^-$ (%) | | 12 (100) | 1 (9.1) | 10 (55.6) |
| Serum IgE level 3 (%) (range: ≥200 IU/ml) | 10 (50.0) | 1 (8.3) | 11 (100) | |
| Serum IgE level 2 (%) (range: 100–199 IU/ml) | 2 (10.0) | 1 (8.3) | | |
| Serum IgE level 1 (%) (range: 0–99 IU/ml) | 8 (40.0) | 10 (83.3) | | 18 (100) |
| Age range, yrs | 18–57 | 18–52 | 19–57 | 18–52 |
| Mean age, yrs (SEM) | 29.2 (±2.6) | 35.0 (±3.1) | 32.2 (±4.1) | 32.8 (±2.5) |
| No. of allergens positive for MAST[b,d] | 2.7 (±0.2) | | 3.3 (±0.3) | 2.0 (±0.4) |
| Mean levels of MAST reactivity[b,e] | 3.7 (±0.2) | | 4.3 (±0.3) | 2.9 (±0.5) |

[a]All subjects ($n = 32$) were tested for both AR and total serum IgE levels.
[b]Only MAST-positive participants were considered.
[c]Subjects showing IgE level 3 and IgE level 1 were considered $IgE^{high}$ and $IgE^{low}$, respectively. The three patients with IgE level 2 were omitted for comparative analysis between the IgE groups.
[d]A significant difference ($P = 0.016$) was observed between the IgE groups (values of $<0.05$ were considered to indicate significant difference).
[e]A significant difference ($P = 0.011$) was observed between the IgE groups.

taxa (Fig. S2D and E), suggesting that AR occurrence itself was not sufficient for alpha- or beta-diversity dysbiosis in inferior turbinate mucosa microbiota. Sex or age specificity of the inferior turbinate microbiota was not observed (data not shown).

**Association of the number of sensitized allergens with the inferior turbinate mucosa microbiota.** AR patients sensitized to multiple allergens (polysensitization) are known to have more inflammation and severe symptoms than those who are sensitized to a single allergen (monosensitization) (20). AR subjects in our cohorts were sensitized to one to five allergens (Table S1). To investigate the inferior turbinate microbiota according to the number of sensitized allergens, we compared microbiota among three groups categorized into three sensitization patterns as follows: (i) not sensitized to any tested allergens (no-sensitization group), (ii) sensitized to only one allergen (monosensitization group), and (iii) sensitized to multiple allergens (polysensitization group). There were no differences in microbial diversity or community composition among the three groups (Fig. S3). We further correlated microbiota with the continuous values of the number of sensitized allergens. The number of sensitized allergens was not significantly associated with microbial community separation ($R^2 = 0.11$ and $P = 0.08$) and microbial diversity ($R^2 = 0.09$ and $P = 0.06$). Taken together, these results suggested that the number of sensitized allergens was not a direct determinant for alteration or dysbiosis of inferior turbinate mucosa microbiota.

**Comparison of the inferior turbinate mucosal microbiota according to serum IgE-based allergen sensitivity levels.** We hypothesized that the inferior turbinate microbiota was affected by levels of allergen sensitivity rather than the number of sensitized allergens. We classified allergen sensitivity into individual allergen sensitivity (individual allergen-specific IgE levels) and combined sensitivity against all sensitized allergens (total IgE levels). To identify which individual allergen-specific IgE levels were associated with the inferior turbinate microbiota in AR patients, we categorized subjects into three groups according to specific IgE levels against house dust mite allergens (allergic reaction observed in >90% of AR patients [Table S1]) as follows: (i) low level (0 to 0.69 IU/ml) (group Mite-$IgE^{low}$), (ii) intermediate level (0.7 to 17.49 IU/ml) (group Mite-$IgE^{med}$), and (iii) high level (≥17.5 IU/ml) (group Mite-$IgE^{high}$). Although lower microbial diversity was observed in the Mite-$IgE^{high}$ group, the overall composition of the microbial community in the inferior turbinate was not significantly different among the three groups, suggesting that individual allergen specific-IgE levels did not separately affect the inferior turbinate microbiota (Fig. S4).

**TABLE 2** Group categorization according to AR occurrence and total IgE levels

| Parameter | Value for group | | |
|---|---|---|---|
| | AR−IgE$^{low}$ | AR+IgE$^{low}$ | AR+IgE$^{high}$ |
| No. of subjects[a] | 10 | 8 | 10 |
| Male (%) | 6 (60.0) | 5 (62.5) | 9 (90.0) |
| Female (%) | 4 (40.0) | 3 (37.5) | 1 (10.0) |
| SPT$^+$ and MAST$^+$ (%) | | 8 (100) | 10 (100) |
| SPT$^-$ and MAST$^-$ (%) | 10 (100) | | |
| Serum IgE level 3 (%) (range: ≥200 IU/ml) | | | 10 (100) |
| Serum IgE level 1 (%) (range: 0–99 IU/ml) | 10 (100) | 8 (100) | |
| Age range, yrs | 18–52 | 18–42 | 19–57 |
| Mean age, yrs (SEM) | 36.0 (±3.5) | 28.8 (±3.1) | 31.6 (±4.5) |
| No. of subjects positive for multiple allergens (%) | | 5 (62.5) | 10 (100) |
| No. of allergens positive by MAST (range)[b] | | 1–4 | 2–5 |
| Mean no. of allergens positive by MAST[b,e] (SEM) | | 2.0 (±0.4) | 3.3 (±0.3) |
| Mean of avg MAST reactivity levels[c,f] (SEM) | | 3.0 (±0.5) | 4.2 (±0.3) |
| Mean of sum of MAST reactivity levels[d,g] (SEM) | | 5.8 (±1.3) | 14.1 (±1.4) |

[a]Twenty-eight of the 32 subjects were tested for analysis. The three subjects showing IgE level 2 and one subject showing negative SPT and MAST and IgE$^{high}$ (AR−IgE$^{high}$) results were excluded.
[b]Number of positively reactive allergens in MAST.
[c]Average of allergen reactivity levels in each subject based on allergen specific-IgE levels.
[d]Sum of allergen reactivity levels of all positively reactive allergens.
[e]A significant difference ($P = 0.016$) was observed between the AR+IgE$^{low}$ and AR+IgE$^{high}$ groups (values of <0.05 were considered to indicate significant difference).
[f]For the difference between the AR+IgE$^{low}$ and AR+IgE$^{high}$ groups, $P = 0.045$.
[g]A significant difference ($P < 0.001$) was observed between the AR+IgE$^{low}$ and AR+IgE$^{high}$ groups.

Polysensitization is a frequent phenomenon in clinical practice (20). In our study cohort, most (17 of 20) persistent AR patients were sensitive to multiple allergens. We assumed that combined allergic responses from multiple sensitized allergens caused by polysensitization could affect disease phenotype and be used to discriminate the inferior turbinate microbiota in AR patients. In our study cohort, total serum IgE levels were positively correlated with a sum of specific IgE levels of each sensitized allergen ($R^2 = 0.52$ and $P < 0.001$) as well as the number of sensitized allergens ($R^2 = 0.43$ and $P < 0.001$), indicating that total IgE levels reflect combined allergen sensitivity levels. Participants were divided into groups according to total serum IgE levels as follows: IgE level 3 (≥200 IU/ml [IgE$^{high}$]; $n = 11$) and IgE level 1 (0 to 99 IU/ml [IgE$^{low}$]; $n = 18$) (Table 1). Principal-coordinate analyses (PCA) revealed significant separation between two clusters according to total IgE levels (analysis of similarity [ANOSIM], $P = 0.001$) (Fig. 1B), indicating that the inferior turbinate microbiota in subjects with high total IgE levels was different from that in subjects with low total IgE levels. To further clarify the association between the inferior turbinate microbiota and total IgE levels, but not AR occurrence, we compared the microbiota among the following three groups: AR/total serum IgE level 3 (AR+IgE$^{high}$), AR/total serum IgE level 1 (AR+IgE$^{low}$), and non-AR/total serum IgE level 1 (AR−IgE$^{low}$) (Table 2). We found that the microbiota in group AR+IgE$^{high}$ was significantly different from those in groups AR+IgE$^{low}$ and AR−IgE$^{low}$ (ANOSIM, $P < 0.01$) (Fig. S5A and B). However, the microbiota of group AR+IgE$^{low}$ was not significantly different from that of group AR−IgE$^{low}$ (Fig. S5C). Microbial differences were clearer when viewed in terms of total IgE levels rather than AR development (Fig. 1C; see also Fig. S5D to F). Taken together, these data suggest that high levels of total IgE are associated with alterations in the inferior turbinate mucosa microbiota in AR patients.

**Low biodiversity of the inferior turbinate mucosa microbiota in the high total IgE group.** A previous study reported a reduction in skin microbial diversity in individuals with high IgE levels (21). Both bacterial diversity and richness were significantly greater in group IgE$^{low}$ than in group IgE$^{high}$ (Fig. 1D). Similarly, bacterial diversity was significantly greater in groups AR+IgE$^{low}$ and AR−IgE$^{low}$ than in group AR+IgE$^{high}$ (Fig. S6A). Correlation analysis revealed that total IgE levels were negatively correlated with bacterial diversity and richness ($R^2 = 0.219$ and $P = 0.006$ and $R^2 =$

0.244 and $P = 0.004$, respectively). These results suggested that a reduction in the biodiversity of the inferior turbinate mucosa microbiota is associated with high total IgE levels.

**Phylum-level changes in the inferior turbinate mucosa microbial community in the presence of high total IgE levels.** We next examined differences in the composition of the inferior turbinate microbiota in subjects with high and low levels of total IgE. Four bacterial phyla, *Firmicutes*, *Actinobacteria*, *Proteobacteria*, and *Bacteroidetes*, were dominant in groups $IgE^{low}$ and $IgE^{high}$; however, the relative abundances of these phyla in groups $IgE^{low}$ and $IgE^{high}$ were markedly different (Fig. 1E; see also Fig. S7). The phylum *Firmicutes* (60.9%) was significantly more abundant in group $IgE^{high}$ than in group $IgE^{low}$, whereas the phyla *Actinobacteria* and *Bacteroidetes* were significantly less abundant (Fig. S7). At the low taxonomic levels, group $IgE^{high}$ showed higher levels of the order *Bacillales* (*Firmicutes*) and lower levels of the genera *Propionibacterium* (*Actinobacteria*) and *Serratia* (*Proteobacteria*) than group $IgE^{low}$ (Fig. S7). These taxa were consistently detected in group AR+$IgE^{high}$ but not in groups AR+$IgE^{low}$ and AR−$IgE^{low}$ (Fig. S6 and S8). These results suggest changes in the composition of the inferior turbinate mucosa microbial community, including alterations in particular bacterial taxa in the presence of high total IgE levels.

**High abundance of *Staphylococcus aureus* and low relative abundance of *Propionibacterium acnes* in the inferior turbinate mucosa microbiota from the high total IgE group.** To characterize key members of the altered inferior turbinate microbiota in group $IgE^{high}$ at the lowest taxonomic level, we selected discriminant operational taxonomic units (OTUs) using relative abundance-based comparison between groups $IgE^{high}$ and $IgE^{low}$. Of these, 36 OTUs (≥0.5%) accounted for an average 74.8% of the OTUs in group $IgE^{low}$ and 89.1% of the OTUs in group $IgE^{high}$. As shown in Fig. 1D, the low diversity of the microbiota in group $IgE^{high}$ may be due to the dominance of a particular OTU, which was identified as a member of the *Staphylococcus* genus (Fig. 2A). OTU 1078527, assigned to type strain *Staphylococcus aureus* subsp. *aureus* with 100% identity in terms of the 16S rRNA gene, was dominant only in group $IgE^{high}$ despite being present in both groups (Fig. 2B and C). Consistent with the 16S rRNA sequencing data, the results of quantitative real-time PCR (qPCR) using primers specific for the *femB* gene of *S. aureus* (22) show that the absolute abundance of *S. aureus* was higher in group $IgE^{high}$ than in group $IgE^{low}$ (Fig. 2B). Because *S. aureus* plays a role in inducing AR and promoting allergic inflammation cascades via its toxins and serine protease-like proteins (23–25), enrichment of *S. aureus* in group $IgE^{high}$ may aggravate AR. In contrast, the amounts of the *Staphylococcus epidermidis*-assigned OTU (99.7% identity) were no different between groups $IgE^{high}$ and $IgE^{low}$ (Fig. 2D). *S. epidermidis* plays a beneficial role in immune defense devoid of inflammation (26). The *Propionibacterium acnes*-assigned OTU (100% identity) was detected in all samples but was more abundant in group $IgE^{low}$ than in group $IgE^{high}$ (Fig. 2C and D). In particular, low levels of the *P. acnes*-assigned OTU in group $IgE^{high}$ were associated with a high susceptibility to AR; this may be because *P. acnes* improves atopic symptoms by inducing $T_H1$ immune responses and Tregs (27). The relative abundance of the OTUs assigned to *Serratia grimesii* (100% identity) was lower in group $IgE^{high}$ than in group $IgE^{low}$ (Fig. 2D). Correlation analysis revealed that *S. aureus* was positively correlated with total IgE levels (Fig. 3), whereas *P. acnes* and *Serratia grimesii* were negatively correlated with total IgE levels and positively correlated with microbial diversity (Fig. 3), indicating that microbial dysbiosis was caused by changes in the populations of particular bacterial taxa. Although the *Corynebacterium accolens*-assigned OTU (99.7% identity) showed a higher relative abundance in group $IgE^{high}$ than $IgE^{low}$, the relative abundance of this OTU was not correlated with total IgE levels or microbial diversity (Fig. 2D and 3). Taken together, these data suggest that an increase in *S. aureus* and a decrease in *P. acnes* are representative features of the altered inferior turbinate mucosa microbiota under high total IgE conditions and that enrichment of allergy-prone *S. aureus* and loss of allergy-protective *P. acnes* might be associated with AR aggravation.

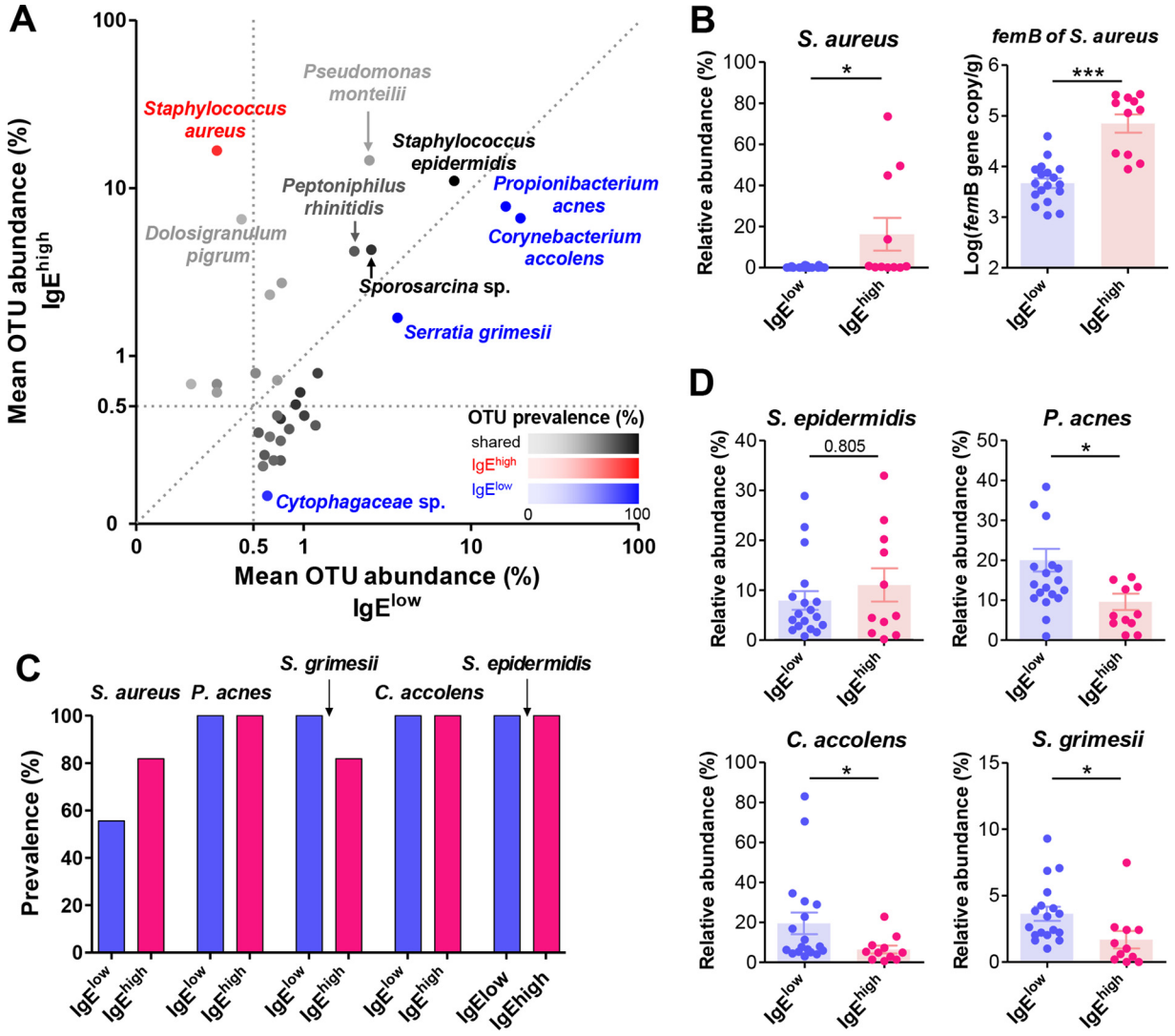


**FIG 2** OTUs that discriminate between two IgE levels, and the predominant OTUs, in the inferior turbinate mucosa microbiota. (A) Each dot represents mean relative abundance of OTUs in group $IgE^{low}$ (*x* axis) and group $IgE^{high}$ (*y* axis). OTUs significantly enriched in group $IgE^{low}$ are shown in blue, while those significantly enriched in group $IgE^{high}$ are shown in red. Nondiscriminant OTUs are shown in black. *P* values of <0.05 indicated significantly discriminant OTUs in both of the two-tailed Mann-Whitney *U* test and the best-fitted statistical test (either the negative binomial model, Poisson model, or zero-inflated negative binomial model). Only OTUs at >0.5% of the total abundance are shown. (B) Comparisons of abundances of *S. aureus*. Two graphs show the mean relative abundance (left) and mean absolute abundance (right) of *S. aureus*, respectively. (C and D) Comparison of prevalences (C) and the mean relative abundances (D) of major bacterial OTUs between groups $IgE^{low}$ and $IgE^{high}$. For panels B and D, *P* values were determined using the two-tailed Mann-Whitney *U* test. *, $P < 0.05$; ***, $P < 0.001$.

The overall community composition of the inferior turbinate mucosa microbiota is shown in Fig. 1E and Fig. S9.

**Altered microbial functional potential in the inferior turbinate mucosa from the high total IgE group.** To determine differences in the functional potential of the inferior turbinate microbiota from the different groups, we predicted the metagenomes of the inferior turbinate microbiota using a 16S rRNA gene data set and compared differences in predicted functional gene abundance with Kyoto Encyclopedia of Genes and Genomes (KEGG) orthologs using PICRUSt (28). We found significant differences of functional potential in the total IgE group (ANOSIM, $P = 0.003$) (Fig. 4A and B). To identify the predicted microbial functional genes that differed between groups $IgE^{high}$ and $IgE^{low}$, we then compared the relative abundances of 268 KEGG orthology groups (KOs). At the first level of KO hierarchy, we found that group $IgE^{high}$ showed higher relative abundances of two KOs related to human disease and environmental informa-

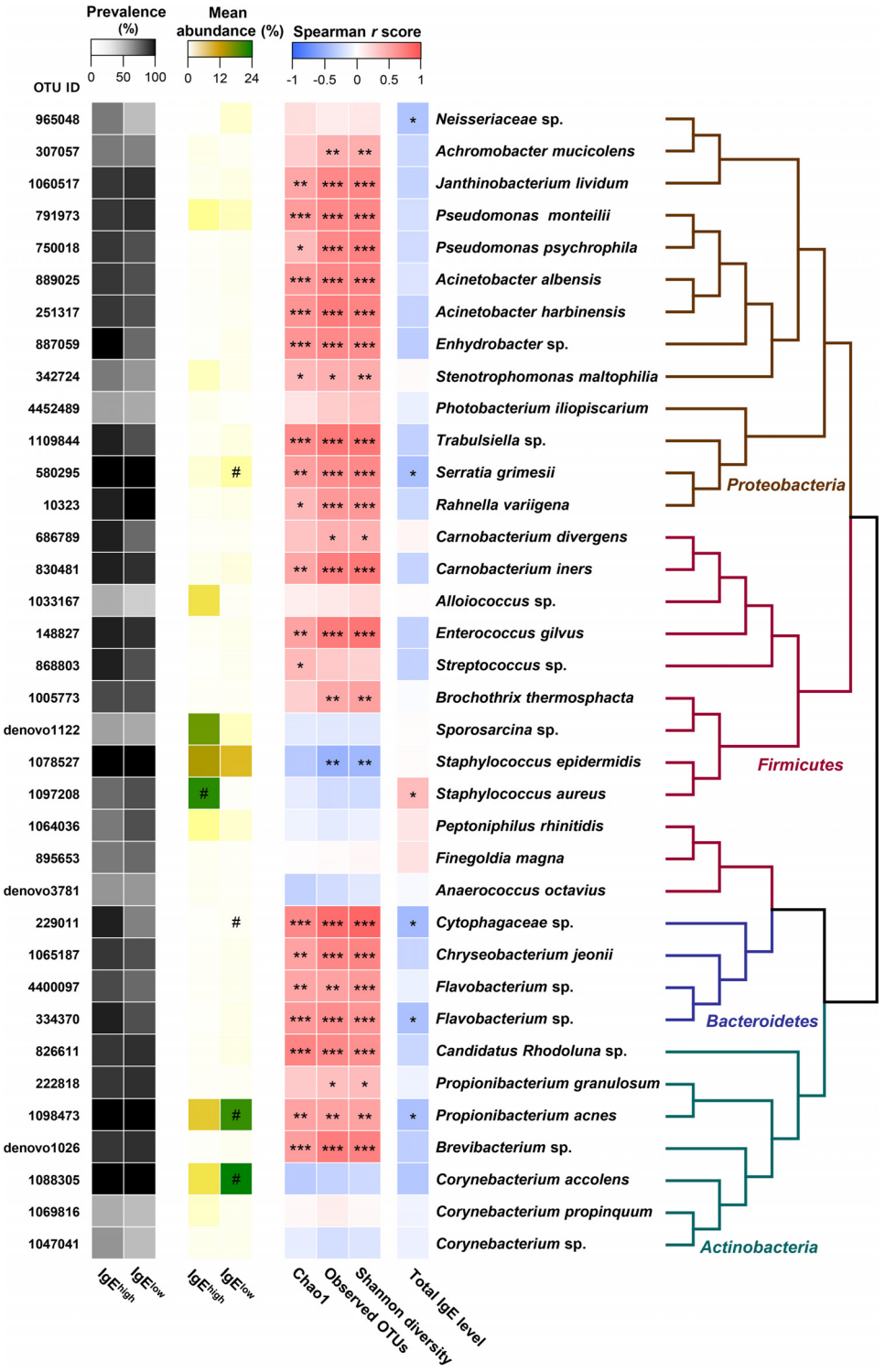


**FIG 3** Correlation between the relative abundance of major OTUs and total IgE levels and microbial diversity indices (Spearman's correlation analysis). The heat maps shown in yellow to green and white to black depict the mean relative abundances and prevalences, respectively, of the major OTUs. In the heat map showing relative abundance, the OTUs that discriminate between the two IgE groups are marked by a pound sign. The heat map in blue to red shows the correlation scores (*rho*) between the relative abundances of major OTUs and total IgE levels and between the relative abundance of major OTUs and microbial diversity. In the heat map showing the correlation scores, significant *P* values are indicated by asterisks. A phylogenetic tree based on 16S rRNA gene sequences for each OTU shows the taxonomic position of the major OTUs. #, $P < 0.05$; *, $P < 0.05$; **, $P < 0.01$; ***, $P < 0.001$.

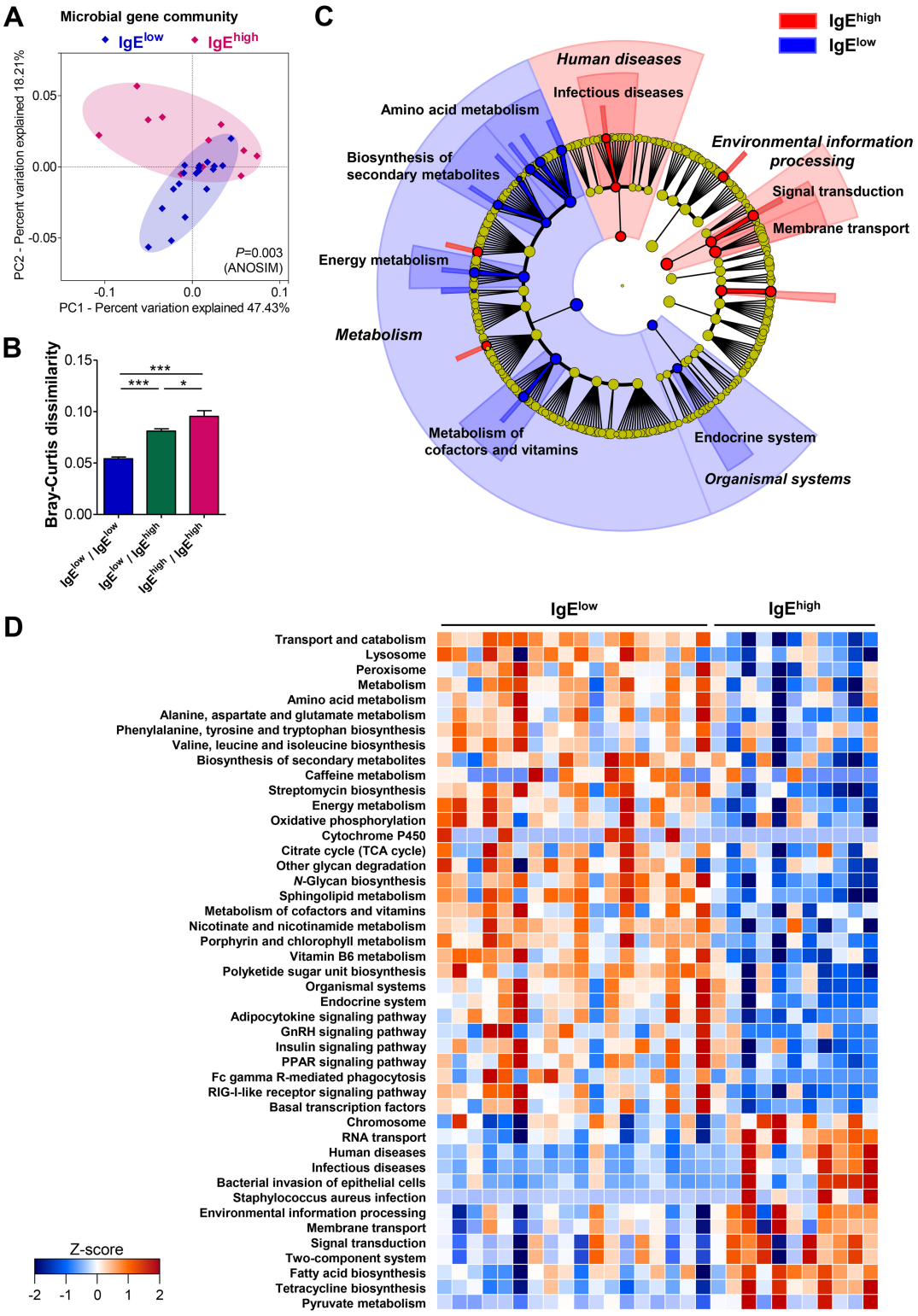


**FIG 4** Effect of IgE levels on the gene community of the inferior turbinate mucosa microbiota and the microbial gene characteristics that discriminate between $IgE^{high}$ and $IgE^{low}$ groups. (A) Principal-coordinate analysis of Bray-Curtis dissimilarities in the inferior turbinate microbial gene community. Each point represents an individual predicted microbial functional gene community. (B) Average Bray-Curtis dissimilarities representing intragroup and intergroup variability within the microbial gene community structure. (C) Cladograms generated by LEfSe analysis. Shaded areas represent gene families that are significantly enriched in group $IgE^{low}$ or group $IgE^{high}$ at the first and second levels of KO hierarchy. (D) Heat map depicting normalized abundance of microbial gene families that discriminate between subjects with different IgE levels. For panels B and D, *P* values were determined by the two-tailed Mann-Whitney *U* test. *, $P < 0.05$; ***, $P < 0.001$. Panel C was generated from the LEfSe analysis.

tion processing, and a lower relative abundance of the KO related to metabolism and organismal systems, than group IgE$^{low}$ (Fig. 4C). At the second level of KO hierarchy, we found that group IgE$^{high}$ showed higher relative abundances of KO families related to infectious diseases, signal transduction, and membrane transport, and lower relative abundances of KO families related to metabolism (i.e., amino acid metabolism, secondary metabolite biosynthesis, energy metabolism, and metabolism of cofactors and vitamins), than group IgE$^{low}$ (Fig. 4C and D). The low relative abundance of KOs (i.e., amino acid metabolism) specific to group IgE$^{high}$ was also observed in the gut microbiome of subjects with FUT2 Crohn's disease (29) and in the skin microbiome of individuals with atopic dermatitis (30). A high relative abundance of KOs (i.e., two-component system of signal transduction) specific to group IgE$^{high}$ was found in cystic fibrosis patients (31). In addition, enrichment or depletion of several KOs, including carbohydrate metabolism, energy metabolism, secondary metabolite biosynthesis (depleted in group IgE$^{high}$), signal transduction, and two-component systems (enriched in group IgE$^{high}$), in group IgE$^{high}$ was consistent with predicted microbial functions in mice with active colitis (32). Taken together, these results indicate that dysbiosis accompanying alteration of microbiota composition and predicted microbial gene content occurs in the inferior turbinate microbiota of patients with high levels of total IgE and that changes in the commensal microbiota within the inferior turbinate may be associated with the pathogenesis and aggravation of AR.

## DISCUSSION

The commensal microbiota plays both regulatory and stimulatory roles during host immune development, and its dysbiosis provokes aberrant immune responses (6, 10). Thus, understanding host-microbe interactions under allergic conditions improves our knowledge of the pathophysiology of AR. However, no study has examined the association between AR pathophysiology and the commensal microbiota in the nasal cavity. In this study, we used 16S rRNA gene-based 454 pyrosequencing to characterize and compare the inferior turbinate mucosa microbiota in healthy controls and AR patients and found that microbial dysbiosis of the inferior turbinate in the latter is associated with high levels of total IgE but not with AR occurrence, the number of sensitized allergens, or house dust mite allergen-specific IgE. This is the first study to characterize the commensal microbiota in the inferior turbinate (the anatomical site of AR), and the results underscore the association between dysbiosis of inferior turbinate microbiota and AR pathogenesis.

Our study found that the inferior turbinate mucosa microbiota was associated not with AR occurrence or the number of sensitized allergens but with combined allergic responses from multiple sensitized allergens (represented as total serum IgE level). In the 20 participants with AR showing differing total serum IgE levels (50% IgE level 3, 10% IgE level 2, and 40% IgE level 1), all but one of the subjects with total serum IgE level 3 was assigned to the AR+ group. Also, microbial dysbiosis specific for high total serum IgE condition was evaluated through multiple comparisons among the AR−IgE$^{low}$, AR+IgE$^{low}$, and AR+IgE$^{high}$ groups. As a result, it is evident that the composition of the inferior turbinate microbiota from the subjects was associated with high total IgE levels in AR. Serum IgE is a diagnostic biomarker and a potential therapeutic target in AR. IgE is secreted by B cells that are stimulated by inhaled allergens; allergen-IgE cross-linking then triggers allergic inflammatory responses (1, 33). Thus, a high IgE level is considered a risk factor for allergen-related symptoms, and it has been experimentally observed in several studies of allergic diseases (6, 15, 34, 35). Recently, Cahenzli et al. found that a gut microbiota with a low level of diversity would lead to increased IgE levels, which cause systemic anaphylaxis; however, a highly diverse gut microbiota does not lead to hyper-IgE (36). Similarly, we found that low bacterial diversity within the inferior turbinate microbiota was associated with high total IgE levels. Taken together, these results support a connection between the commensal microbiota and total IgE levels in AR.

We noted marked phylum-level changes in the inferior turbinate microbiota in those

with high IgE levels. Unlike the microbial pattern of the inferior turbinate microbiota noted in healthy individuals, both previously (37, 38) and in this study, the *Firmicutes* phylum was dominant in the inferior turbinate microbiota of AR patients under high IgE conditions, a condition attributable to low diversity of the inferior turbinate microbiota. Phylum-level alterations are a widely used marker of microbial dysbiosis related to human health and disease (39); therefore, this finding may be a disease-specific microbial characteristic of the inferior turbinate environment related to allergic diseases, including AR, although further studies are needed to support this notion.

Individual members of the commensal microbiota are *per se* expected to have different immunomodulatory effects in terms of occurrence and progression of allergic disease. In this study, we observed a high abundance of *S. aureus* and a low relative abundance of *P. acnes* in the altered inferior turbinate microbiota of AR patients with high levels of total IgE. *S. aureus* induces IgE production and promotes allergic inflammation (23, 24). Conversely, high IgE levels elicit a bloom of *S. aureus*, which activates mast cell degranulation and contributes to inflammation (21, 39). Furthermore, *S. aureus* is known to proliferate in disrupted skin microbiota in atopic dermatitis (40). In this context, we suppose that allergy-prone *S. aureus* and IgE may enter a positive-feedback loop in AR patients with high IgE levels, thereby making both an individual contribution to allergic inflammation and a synergistic contribution when a bloom of *S. aureus* organisms occurs. Thus, controlling the levels of both *S. aureus* and IgE may be an effective strategy for preventing IgE-associated diseases, including AR. *P. acnes* is predominant within the inferior turbinate bacteria population in healthy individuals (41) and improves atopic symptoms by inducing $T_H1$ and Treg responses (27); this implies that a low abundance of *P. acnes* may be associated with AR aggravation. Our findings suggest that dominant members of the inferior turbinate bacteria might be involved in AR progression in individuals with high levels of total IgE.

Consistent with alterations in the composition of the inferior turbinate mucosa microbiota, we also found alterations of predicted functional genes in subjects with high IgE levels. The profiles of predicted microbial genes in subjects with high IgE levels differed from those in subjects with low levels. Notably, alterations of predicted functions similar to those found in the commensal microbiota of individuals with Crohn's disease, atopic dermatitis, and cystic fibrosis were observed in the inferior turbinate microbiota of subjects with high IgE levels (29–31); this implies that disease-specific functional features of the inferior turbinate microbiota may contribute to AR pathophysiology. Polyphasic approaches are needed to better define the functional interactions between the host and commensal microbiota.

In summary, we showed that alterations toward to dysbiosis in the composition and predicted function of the inferior turbinate microbiota in individuals with AR are associated with high total IgE levels. Importantly, the dominance of *S. aureus*, known to promote allergic inflammation, in the altered microbiota suggests that microbial dysbiosis in inferior turbinate microbiota may play an important role in AR development and progression. This study will help us to understand how the nasal microbiota in the inferior turbinate environment interacts with the host immune system. Furthermore, our findings are preliminary; thus, further studies of microbial dysbiosis in the upper airway may yield new therapeutic approaches to the management of AR.

## MATERIALS AND METHODS

**Study design and sample collection.** The study was approved by the institutional review board (IRB) of the Yonsei University College of Medicine (4-2014-0114), and all participants provided informed consent. A total of 32 subjects (24 men and 8 women), all of whom who underwent septoplasty, were enrolled, and all met the following criteria: (i) ≥18 years of age, (ii) receiving no immunotherapy, (iii) no chronic rhinosinusitis confirmed by computed tomography scans, (iv) not pregnant or breast-feeding, (v) not diagnosed with malignant neoplasm, (vi) no history of nasal surgery, (vii) no history of allergic skin diseases and allergic asthma, and (viii) receiving no medication for the treatment of allergic diseases, including AR, during the previous 2 months (Fig. S1). Next, the subjects were tested to confirm an AR diagnosis. AR ($n = 20$) was diagnosed when patients fulfilled the following criteria: (i) presenting with persistent rhinitis symptoms (more than 4 days per week and more than 4 weeks) for over 1 year (according to ARIA) (42), (ii) a positive SPT

(wheal diameter ≥3 mm larger than that of negative control after 15 min) to at least one allergen, and (iii) high titer (≥2 positivity; ≥0.70 IU/ml) of IgE antibodies specific for *Dermatophagoides farina*, *Dermatophagoides pteronyssinus*, house dust mite, animal dander, or mold (like *Aspergillus*) in the MAST (43) (Fig. S1). Participants ($n = 12$) (i) presenting with no symptoms of clinical rhinitis, such as chronic sneezing and watery rhinorrhea, (ii) negative by the SPT, and (iii) with the lowest levels (<1 positivity; 0 to 0.34 IU/ml) of allergen specific-IgE antibodies in the MAST were considered healthy. Total and allergen-specific IgE was measured using Advansure Allostation (LG). All patients in this study were allergic either to perennial allergens or to both seasonal and perennial allergens (Table S1). Patients allergic to seasonal allergens alone were excluded. Inferior turbinate biopsy specimens were taken under general anesthesia at the Department of Otorhinolaryngology, Severance Hospital, from May 2014 to May 2015. A section of inferior turbinate tissue (Fig. 1A) (about 5 by 5 mm) was harvested as previously described (44) and immediately frozen at −80°C. Group categorization, MAST reactivity, total serum IgE levels, and general patient characteristics are shown in Table S1.

**DNA extraction, 16S rRNA gene amplification, and pyrosequencing.** Microbial genomic DNA was extracted from the inferior turbinate biopsy specimens using the repeated-bead beating method (45). The V1-V2 region of the 16S rRNA gene was amplified using barcoded forward primer 27F (5′-XXXXXX XXXX-GAGTTTGATCMTGGCTCAG-3′, where "X" represents the barcode sequence) with an FLX Titanium adapter, and reverse primer 338R (5′-TGCTGCCTCCCGTAGGAGT-3′) with an FLX Titanium adapter. PCR mixtures contained 8 μl of diluted DNA template (1:7), 2 μl of primer mix (0.2 μM), and 2× *Ex Taq* polymerase premix (TaKaRa) in a total reaction volume of 50 μl. PCR conditions were as follows: initial denaturation at 94°C for 3 min, 28 cycles of denaturation at 94°C for 30 s, annealing at 55°C for 45 s, and elongation at 72°C for 60 s, with a final elongation step at 72°C for 8 min. Amplicons were prepared as eight replicates and purified using a QIAquick PCR purification kit (Qiagen). DNA concentration was measured using a Quant-iT PicoGreen double-stranded DNA (dsDNA) kit (Invitrogen). The amplicons were pooled in equimolar concentrations. Pyrosequencing was performed on a 454 GS-FLX Titanium sequencing platform (Roche).

**Analysis of the inferior turbinate mucosa microbiota.** A total of 275,826 raw reads were obtained. The reads were quality filtered and analyzed using the QIIME platform (46). Picking of operational taxonomic units (OTUs) (≥97% identity) was performed against the Greengenes database (2013-08) (47). Taxonomy was assigned using the RDP classifier against the Greengenes database (47). Unassigned or non-bacterial kingdom-assigned sequences and singletons were excluded. Finally, 100,943 high-quality reads (3,145 ± 57 reads per sample) were obtained. From the high-quality reads, each sample was rarefied to 495 sequences to minimize potential bias due to uneven sequencing depth. Alpha-diversity was then determined using the Shannon diversity index, Chao1, and observed OTUs. Beta-diversity was determined using PCA on the basis of weighted UniFrac and Bray-Curtis distances. Profiles of microbial functional potential were analyzed using PICRUSt (28). Functional gene families were predicted based on KEGG orthology groups (48). The predicted functional gene data set was subsampled to 200,000 KOs. Details are provided in the supplemental material.

**Quantification of *S. aureus* organisms in the inferior turbinate mucosa.** The absolute abundance of *S. aureus* in the inferior turbinate mucosa was estimated by qPCR using primers specific for the *femB* gene of *S. aureus* (22). Standard curves were generated by plotting the threshold cycle (49) against PCR products amplified from genomic DNA derived from an *S. aureus* isolate from the human inferior turbinate. The gene copy number in a known amount of amplified DNA was calculated as described previously (50). Details are provided in the supplemental material.

**Statistical analysis.** The statistical significance of the different taxonomic and predicted functional features between groups was determined using two-tailed Mann-Whitney *U* test. Furthermore, taxonomic and predicted functional characteristics that were deemed significantly different between groups by the Mann-Whitney *U* test were analyzed using the best of three models: a negative binomial model (NB), a Poisson model, or a zero-inflated negative binomial model (ZINB). The best statistical model was selected using NegBinSig-Test (https://github.com/alifar76/NegBinSig-Test) based on Bayesian information criteria. Characteristics showing significance in both of the two statistical tests (Mann-Whitney *U* test and the suggested best statistical model [either the NB, Poisson, or ZINB]) were considered significant. Also, discriminant taxonomic and predicted functional characteristics between groups were determined using the linear discriminant effect size (LEfSe) analysis (https://huttenhower.sph.harvard.edu/galaxy/) (51). Correlation analysis was performed using Spearman's rank correlation coefficient. The statistical analyses, two-tailed Mann-Whitney *U* test and Spearman's rank correlation, were performed using GraphPad Prism software (version 5.0; GraphPad Software). Differences between microbial communities and predicted microbial functional gene profiles between groups were statistically tested using ANOSIM methods. *P* values of <0.05 were considered statistically significant. Data are expressed as the means ± standard errors of the means (SEMs).

**Accession number(s).** The metagenome sequences used for this study have been deposited into the European Nucleotide Archive (ENA) of EMBL-EBI under EMBL accession number PRJEB14731 (ERP016397).

## SUPPLEMENTAL MATERIAL

Supplemental material for this article may be found at https://doi.org/10.1128/IAI.00934-17.

**SUPPLEMENTAL FILE 1,** PDF file, 0.1 MB.

**SUPPLEMENTAL FILE 2,** PDF file, 0.3 MB.
**SUPPLEMENTAL FILE 3,** PDF file, 0.5 MB.
**SUPPLEMENTAL FILE 4,** PDF file, 0.5 MB.
**SUPPLEMENTAL FILE 5,** PDF file, 0.5 MB.
**SUPPLEMENTAL FILE 6,** PDF file, 0.6 MB.
**SUPPLEMENTAL FILE 7,** PDF file, 0.5 MB.
**SUPPLEMENTAL FILE 8,** PDF file, 1.0 MB.
**SUPPLEMENTAL FILE 9,** PDF file, 0.3 MB.
**SUPPLEMENTAL FILE 10,** PDF file, 0.2 MB.

## ACKNOWLEDGMENTS

This work was supported by the Collaborative Genome Program for Fostering New Post-Genome industry (2015M3C9A2054299), Global Research Lab program (2016K1A1A2910779), and Mid-career Researcher Program (2016R1E1A1A02921587) through the National Research Foundation of Korea (NRF) funded by the Ministry of Science ICT & Future Planning.

We declare no conflict of interest.

## REFERENCES

1. Galli SJ, Tsai M, Piliponsky AM. 2008. The development of allergic inflammation. Nature 454:445–454. https://doi.org/10.1038/nature07204.
2. Sin B, Togias A. 2011. Pathophysiology of allergic and nonallergic rhinitis. Proc Am Thorac Soc 8:106–114. https://doi.org/10.1513/pats.201008-057RN.
3. Cruz AA, Bousquet J, Khaltaev N. 2007. Global surveillance, prevention and control of chronic respiratory diseases: a comprehensive approach. World Health Organization, Geneva, Switzerland.
4. Strachan DP. 1989. Hay fever, hygiene, and household size. BMJ 299:1259–1260. https://doi.org/10.1136/bmj.299.6710.1259.
5. Wills-Karp M, Santeliz J, Karp CL. 2001. The germless theory of allergic disease: revisiting the hygiene hypothesis. Nat Rev Immunol 1:69–75. https://doi.org/10.1038/35095579.
6. Hill DA, Siracusa MC, Abt MC, Kim BS, Kobuley D, Kubo M, Kambayashi T, Larosa DF, Renner ED, Orange JS, Bushman FD, Artis D. 2012. Commensal bacteria-derived signals regulate basophil hematopoiesis and allergic inflammation. Nat Med 18:538–546. https://doi.org/10.1038/nm.2657.
7. Round JL, Mazmanian SK. 2009. The gut microbiota shapes intestinal immune responses during health and disease. Nat Rev Immunol 9:313–323. https://doi.org/10.1038/nri2515.
8. Spor A, Koren O, Ley R. 2011. Unravelling the effects of the environment and host genotype on the gut microbiome. Nat Rev Microbiol 9:279–290. https://doi.org/10.1038/nrmicro2540.
9. Turnbaugh PJ, Quince C, Faith JJ, McHardy AC, Yatsunenko T, Niazi F, Affourtit J, Egholm M, Henrissat B, Knight R, Gordon JI. 2010. Organismal, genetic, and transcriptional variation in the deeply sequenced gut microbiomes of identical twins. Proc Natl Acad Sci U S A 107:7503–7508. https://doi.org/10.1073/pnas.1002355107.
10. Lee YK, Mazmanian SK. 2010. Has the microbiota played a critical role in the evolution of the adaptive immune system? Science 330:1768–1773. https://doi.org/10.1126/science.1195568.
11. von Mutius E. 2016. The microbial environment and its influence on asthma prevention in early life. J Allergy Clin Immunol 137:680–689. https://doi.org/10.1016/j.jaci.2015.12.1301.
12. Nylund L, Nermes M, Isolauri E, Salminen S, de Vos WM, Satokari R. 2015. Severity of atopic disease inversely correlates with intestinal microbiota diversity and butyrate-producing bacteria. Allergy 70:241–244. https://doi.org/10.1111/all.12549.
13. Ohnmacht C, Park JH, Cording S, Wing JB, Atarashi K, Obata Y, Gaboriau-Routhiau V, Marques R, Dulauroy S, Fedoseeva M, Busslinger M, Cerf-Bensussan N, Boneca IG, Voehringer D, Hase K, Honda K, Sakaguchi S, Eberl G. 2015. The microbiota regulates type 2 immunity through ROR-gammat(+) T cells. Science 349:989–993.
14. Schwarzer M, Repa A, Daniel C, Schabussova I, Hrncir T, Pot B, Stepankova R, Hudcovic T, Pollak A, Tlaskalova-Hogenova H, Wiedermann U, Kozakova H. 2011. Neonatal colonization of mice with *Lactobacillus plantarum* producing the aeroallergen Bet v 1 biases towards Th1 and T-regulatory responses upon systemic sensitization. Allergy 66:368–375. https://doi.org/10.1111/j.1398-9995.2010.02488.x.
15. Stefka AT, Feehley T, Tripathi P, Qiu J, McCoy K, Mazmanian SK, Tjota MY, Seo GY, Cao S, Theriault BR, Antonopoulos DA, Zhou L, Chang EB, Fu YX, Nagler CR. 2014. Commensal bacteria protect against food allergen sensitization. Proc Natl Acad Sci U S A 111:13145–13150. https://doi.org/10.1073/pnas.1412008111.
16. Kim YG, Udayanga KG, Totsuka N, Weinberg JB, Nunez G, Shibuya A. 2014. Gut dysbiosis promotes M2 macrophage polarization and allergic airway inflammation via fungi-induced PGE(2). Cell Host Microbe 15:95–102. https://doi.org/10.1016/j.chom.2013.12.010.
17. Chhabra N, Houser SM. 2014. Surgery for allergic rhinitis. Int Forum Allergy Rhinol 4(Suppl 2):S79–S83. https://doi.org/10.1002/alr.21387.
18. Liu Z, Tan JL, Cohen DM, Yang MT, Sniadecki NJ, Ruiz SA, Nelson CM, Chen CS. 2010. Mechanical tugging force regulates the size of cell-cell junctions. Proc Natl Acad Sci U S A 107:9944–9949. https://doi.org/10.1073/pnas.0914547107.
19. Hupin C, Gohy S, Bouzin C, Lecocq M, Polette M, Pilette C. 2014. Features of mesenchymal transition in the airway epithelium from chronic rhinosinusitis. Allergy 69:1540–1549. https://doi.org/10.1111/all.12503.
20. Gelardi M, Ciprandi G, Incorvaia C, Buttafava S, Leo E, Iannuzzi L, Quaranta N, Frati F. 2015. Allergic rhinitis phenotypes based on mono-allergy or poly-allergy. Inflamm Res 64:373–375. https://doi.org/10.1007/s00011-015-0826-9.
21. Oh J, Freeman AF, Program NCS, Park M, Sokolic R, Candotti F, Holland SM, Segre JA, Kong HH. 2013. The altered landscape of the human skin microbiome in patients with primary immunodeficiencies. Genome Res 23:2103–2114. https://doi.org/10.1101/gr.159467.113.
22. Klotz M, Opper S, Heeg K, Zimmermann S. 2003. Detection of Staphylococcus aureus enterotoxins A to D by real-time fluorescence PCR assay. J Clin Microbiol 41:4683–4687. https://doi.org/10.1128/JCM.41.10.4683-4687.2003.
23. Nakamura Y, Oscherwitz J, Cease KB, Chan SM, Munoz-Planillo R, Hasegawa M, Villaruz AE, Cheung GY, McGavin MJ, Travers JB, Otto M, Inohara N, Nunez G. 2013. *Staphylococcus* delta-toxin induces allergic skin disease by activating mast cells. Nature 503:397–401. https://doi.org/10.1038/nature12655.
24. Okano M, Hattori H, Yoshino T, Sugata Y, Yamamoto M, Fujiwara T, Satoskar AA, Satoskar AR, Nishizaki K. 2005. Nasal exposure to staphylococcal enterotoxin enhances the development of allergic rhinitis in mice. Clin Exp Allergy 35:506–514. https://doi.org/10.1111/j.1365-2222.2005.02195.x.
25. Stentzel S, Teufelberger A, Nordengrun M, Kolata J, Schmidt F, van Crombruggen K, Michalik S, Kumpfmuller J, Tischer S, Schweder T, Hecker M, Engelmann S, Volker U, Krysko O, Bachert C, Broker BM. 2017. Staphylococcal serine protease-like proteins are pacemakers of allergic

airway reactions to Staphylococcus aureus. J Allergy Clin Immunol 139:492–500.e8. https://doi.org/10.1016/j.jaci.2016.03.045.
26. Naik S, Bouladoux N, Linehan JL, Han SJ, Harrison OJ, Wilhelm C, Conlan S, Himmelfarb S, Byrd AL, Deming C, Quinones M, Brenchley JM, Kong HH, Tussiwand R, Murphy KM, Merad M, Segre JA, Belkaid Y. 2015. Commensal-dendritic-cell interaction specifies a unique protective skin immune signature. Nature 520:104–108. https://doi.org/10.1038/nature14052.
27. Kitagawa H, Yamanaka K, Kakeda M, Inada H, Imai Y, Gabazza EC, Kurokawa I, Mizutani H. 2011. *Propionibacterium acnes* vaccination induces regulatory T cells and Th1 immune responses and improves mouse atopic dermatitis. Exp Dermatol 20:157–158. https://doi.org/10.1111/j.1600-0625.2010.01180.x.
28. Langille MG, Zaneveld J, Caporaso JG, McDonald D, Knights D, Reyes JA, Clemente JC, Burkepile DE, Vega Thurber RL, Knight R, Beiko RG, Huttenhower C. 2013. Predictive functional profiling of microbial communities using 16S rRNA marker gene sequences. Nat Biotechnol 31:814–821. https://doi.org/10.1038/nbt.2676.
29. Tong M, McHardy I, Ruegger P, Goudarzi M, Kashyap PC, Haritunians T, Li X, Graeber TG, Schwager E, Huttenhower C, Fornace AJ, Jr, Sonnenburg JL, McGovern DP, Borneman J, Braun J. 2014. Reprograming of gut microbiome energy metabolism by the FUT2 Crohn's disease risk polymorphism. ISME J 8:2193–2206. https://doi.org/10.1038/ismej.2014.64.
30. Song H, Yoo Y, Hwang J, Na YC, Kim HS. 2016. *Faecalibacterium prausnitzii* subspecies-level dysbiosis in the human gut microbiome underlying atopic dermatitis. J Allergy Clin Immunol 137:852–860. https://doi.org/10.1016/j.jaci.2015.08.021.
31. Manor O, Levy R, Pope CE, Hayden HS, Brittnacher MJ, Carr R, Radey MC, Hager KR, Heltshe SL, Ramsey BW, Miller SI, Hoffman LR, Borenstein E. 2016. Metagenomic evidence for taxonomic dysbiosis and functional imbalance in the gastrointestinal tracts of children with cystic fibrosis. Sci Rep 6:22493. https://doi.org/10.1038/srep22493.
32. Rooks MG, Veiga P, Wardwell-Scott LH, Tickle T, Segata N, Michaud M, Gallini CA, Beal C, van Hylckama-Vlieg JE, Ballal SA, Morgan XC, Glickman JN, Gevers D, Huttenhower C, Garrett WS. 2014. Gut microbiome composition and function in experimental colitis during active disease and treatment-induced remission. ISME J 8:1403–1417. https://doi.org/10.1038/ismej.2014.3.
33. Gould HJ, Sutton BJ. 2008. IgE in allergy and asthma today. Nat Rev Immunol 8:205–217. https://doi.org/10.1038/nri2273.
34. Zellweger F, Eggel A. 2016. IgE-associated allergic disorders: recent advances in etiology, diagnosis, and treatment. Allergy 71:1652–1661. https://doi.org/10.1111/all.13059.
35. Olivieri M, Heinrich J, Schlunssen V, Anto JM, Forsberg B, Janson C, Leynaert B, Norback D, Sigsgaard T, Svanes C, Tischer C, Villani S, Jarvis D, Verlato G. 2016. The risk of respiratory symptoms on allergen exposure increases with increasing specific IgE levels. Allergy 71:859–868. https://doi.org/10.1111/all.12841.
36. Cahenzli J, Koller Y, Wyss M, Geuking MB, McCoy KD. 2013. Intestinal microbial diversity during early-life colonization shapes long-term IgE levels. Cell Host Microbe 14:559–570. https://doi.org/10.1016/j.chom.2013.10.004.
37. Bassis CM, Tang AL, Young VB, Pynnonen MA. 2014. The nasal cavity microbiota of healthy adults. Microbiome 2:27. https://doi.org/10.1186/2049-2618-2-27.
38. Yan M, Pamp SJ, Fukuyama J, Hwang PH, Cho DY, Holmes S, Relman DA. 2013. Nasal microenvironments and interspecific interactions influence nasal microbiota complexity and S. aureus carriage. Cell Host Microbe 14:631–640. https://doi.org/10.1016/j.chom.2013.11.005.
39. Kobayashi T, Glatz M, Horiuchi K, Kawasaki H, Akiyama H, Kaplan DH, Kong HH, Amagai M, Nagao K. 2015. Dysbiosis and *Staphylococcus aureus* colonization drives inflammation in atopic dermatitis. Immunity 42:756–766. https://doi.org/10.1016/j.immuni.2015.03.014.
40. Geoghegan JA, Irvine AD, Foster TJ. 9 December 2017. Staphylococcus aureus and atopic dermatitis: a complex and evolving relationship. Trends Microbiol https://doi.org/10.1016/j.tim.2017.11.008.
41. Human Microbiome Project Consortium. 2012. Structure, function and diversity of the healthy human microbiome. Nature 486:207–214. https://doi.org/10.1038/nature11234.
42. Brozek JL, Bousquet J, Baena-Cagnani CE, Bonini S, Canonica GW, Casale TB, van Wijk RG, Ohta K, Zuberbier T, Schunemann HJ, Global Allergy and Asthma European Network, Grading of Recommendations Assessment, Development and Evaluation Working Group. 2010. Allergic Rhinitis and its Impact on Asthma (ARIA) guidelines: 2010 revision. J Allergy Clin Immunol 126:466–476. https://doi.org/10.1016/j.jaci.2010.06.047.
43. Kim JK, Yoon YM, Jang WJ, Choi YJ, Hong SC, Cho JH. 2011. Comparison study between MAST CLA and OPTIGEN. Am J Rhinol Allergy 25:e156–e159. https://doi.org/10.2500/ajra.2011.25.3646.
44. Cho HJ, Lee HJ, Kim SC, Kim K, Kim YS, Kim CH, Lee JG, Yoon JH, Choi JY. 2012. Protease-activated receptor 2-dependent fluid secretion from airway submucosal glands by house dust mite extract. J Allergy Clin Immunol 129:529–535, 535.e1–535.e5. https://doi.org/10.1016/j.jaci.2011.11.024.
45. Yu Z, Morrison M. 2004. Improved extraction of PCR-quality community DNA from digesta and fecal samples. Biotechniques 36:808–812.
46. Caporaso JG, Kuczynski J, Stombaugh J, Bittinger K, Bushman FD, Costello EK, Fierer N, Pena AG, Goodrich JK, Gordon JI, Huttley GA, Kelley ST, Knights D, Koenig JE, Ley RE, Lozupone CA, McDonald D, Muegge BD, Pirrung M, Reeder J, Sevinsky JR, Turnbaugh PJ, Walters WA, Widmann J, Yatsunenko T, Zaneveld J, Knight R. 2010. QIIME allows analysis of high-throughput community sequencing data. Nat Methods 7:335–336. https://doi.org/10.1038/nmeth.f.303.
47. DeSantis TZ, Hugenholtz P, Larsen N, Rojas M, Brodie EL, Keller K, Huber T, Dalevi D, Hu P, Andersen GL. 2006. Greengenes, a chimera-checked 16S rRNA gene database and workbench compatible with ARB. Appl Environ Microbiol 72:5069–5072. https://doi.org/10.1128/AEM.03006-05.
48. Kanehisa M, Goto S, Sato Y, Furumichi M, Tanabe M. 2012. KEGG for integration and interpretation of large-scale molecular data sets. Nucleic Acids Res 40:D109–D114. https://doi.org/10.1093/nar/gkr988.
49. Huse SM, Huber JA, Morrison HG, Sogin ML, Welch DM. 2007. Accuracy and quality of massively parallel DNA pyrosequencing. Genome Biol 8:R143. https://doi.org/10.1186/gb-2007-8-7-r143.
50. Ritalahti KM, Amos BK, Sung Y, Wu Q, Koenigsberg SS, Loffler FE. 2006. Quantitative PCR targeting 16S rRNA and reductive dehalogenase genes simultaneously monitors multiple Dehalococcoides strains. Appl Environ Microbiol 72:2765–2774. https://doi.org/10.1128/AEM.72.4.2765-2774.2006.
51. Segata N, Izard J, Waldron L, Gevers D, Miropolsky L, Garrett WS, Huttenhower C. 2011. Metagenomic biomarker discovery and explanation. Genome Biol 12:R60. https://doi.org/10.1186/gb-2011-12-6-r60.